optica

Electrically pumped random lasers with *p*-diamond as a hole source

Ying-Jie Lu,[1,2] Chong-Xin Shan,[1,3,*] Zhen-Xiang Zhou,[4] Ying-Lei Wang,[5] Bing-Hui Li,[1] Jie-Ming Qin,[6,7] Hong-An Ma,[4] Xiao-Peng Jia,[4] Zhang-Hai Chen,[5] and De-Zhen Shen[1]

[1]State Key Laboratory of Luminescence and Applications, Changchun Institute of Optics, Fine Mechanics and Physics, Chinese Academy of Sciences, Changchun 130033, China
[2]University of Chinese Academy of Sciences, Beijing 100049, China
[3]School of Physical Engineering, Zhengzhou University, 450052 Zhengzhou, China
[4]State Key Laboratory of Superhard Materials, Jilin University, Changchun 130012, China
[5]State Key Laboratory of Surface Physics, Department of Physics, Fudan University, Shanghai 200433, China
[6]School of Materials Science and Engineering, Changchun University of Science and Technology, Changchun 130022, China
[7]School of Physics, Inner Mongolia University for Nationalities, Tongliao 028000, China
*Corresponding author: shancx@ciomp.ac.cn

Received 1 April 2015; revised 10 May 2015; accepted 11 May 2015 (Doc. ID 237357); published 15 June 2015

Electrically pumped lasing has been one of the most challenging issues for random lasers. Since holes are rare in most semiconductors, hole injection is necessary for electrically pumped lasers. Here in this article, by employing *p*-type diamond synthesized via a temperature gradient method under high-pressure and high-temperature conditions as a hole source, electrically pumped random lasing has been observed from *p*-$Mg_{0.35}Zn_{0.65}O$/*n*-ZnO core–shell nanowire structures. The mechanism for the lasing can be attributed to the recombination of the electrons in the nanowires with the holes injected from the *p*-type diamond.

OCIS codes: (250.0250) Optoelectronics; (250.5960) Semiconductor lasers; (160.4236) Nanomaterials; (220.4241) Nanostructure fabrication.

http://dx.doi.org/10.1364/OPTICA.2.000558

1. INTRODUCTION

Random lasing has attracted much attention in the past decades for its various potential applications in displaying, sensing, biological imaging, etc. [1–6]. To date, optically pumped random lasers have been reported extensively [7–12]. To realize electrically pumped random lasing is one of the major issues for the further development and future applications of this kind of laser. Zinc oxide (ZnO) is one of the most promising candidates for use in electrically pumped random lasers for its direct bandgap and relatively large exciton binding energy [13–17]. Nevertheless, to realize electrically pumped emissions, both electrons and holes are needed. While ZnO is intrinsically of *n*-type conduction, that is, electrons are usually sufficient, holes are lacking in this kind of material. Thus, hole injection is necessary to realize electrically pumped random lasers. A natural way to introduce holes is to dope the intrinsic *n*-type ZnO to a *p*-type one. Although some progress has been achieved with *p*-type doping of ZnO [18–20], the realization of efficient *p*-type ZnO is still a challenging issue. Under such a circumstance, how to realize efficient generation and injection of holes into the active layer has been one of the vital issues for electrically pumped random lasers.

Diamond has recently been highlighted for its potential applications in electronic devices, including high-frequency field-effect transistors, high-power switches, Schottky diodes, etc. [21–24]. It is accepted that diamond can be doped into highly hole-dominant conduction, and it is reported that by using boron as a dopant, *p*-type diamond with hole concentration over 10^{18} cm^{-3} can be achieved [25,26]. If *p*-type diamond with such a high hole concentration can be employed as a hole source, electrically pumped random lasers could be produced. However, no such report can be found up to now.

In this article, boron-doped *p*-type diamond has been synthesized via a temperature gradient method under high-temperature and high-pressure conditions and the hole concentration of the diamond is around 3.6×10^{18} cm^{-3}. The diamond has been employed as a hole source for a *p*-$Mg_{0.35}Zn_{0.65}O$/*n*-ZnO core–shell nanowire structure via a direct contact route. Random lasers with well-defined sharp peaks have been observed, and the random laser can be attributed to the recombination of the electrons in *n*-ZnO with the holes injected from the *p*-type diamond.

2. EXPERIMENTAL

The *p*-type boron-doped diamond was synthesized in a cubic anvil high-pressure apparatus at ~5.5 GPa and ~1300°C. Graphite (99.99%) was used as the carbon source and

$Ni_{70}Mn_{25}Co_5$ alloy was adopted as the solvent. Amorphous boron (99.9%) powder was used as additive to prepare the boron-doped diamond and the boron content is about 0.5 wt. %. Diamond crystallites (about 0.6 mm in size) obtained by the chemical vapor deposition method were used as the seed for the preparation of the boron-doped diamond and the (111) facet of the seed was used as the nucleate surface. A boron-doped diamond about 3 mm in size was synthesized by the temperature gradient method after 24 h. The diamond was cut into a plate with a thickness of around 1 mm. To obtain smooth surfaces, the plate was polished on both sides. The ZnO nanowires employed as the active layer for the random lasers were grown on *a*-plane sapphire substrate by a metal-organic chemical vapor deposition technique. Diethylzinc and oxygen were used as the precursors for the growth of the ZnO nanowires. High-purity (9N) nitrogen was employed as the carrier gas to lead the precursors into the growth chamber. The substrate temperature was kept at 650°C and the pressure in the growth chamber was kept at 3×10^3 Pa during the growth process. The *p*-$Mg_{0.35}Zn_{0.65}O$ layers were grown by the plasma-assisted molecular beam epitaxy technique (VG V80H) using a lithium and nitrogen codoping method [27–29] employing high-purity elemental zinc, magnesium, and lithium contained in Knudsen cells as Zn, Mg, and Li sources, respectively, and atomic oxygen and nitrogen generated from O_2 and NO gases via 13.56 MHz radio frequency plasma cells operated at 300 W as O and N sources, respectively. During the growth process, the pressure in the growth chamber was fixed at 2×10^{-5} mbar and the O_2 and NO flow rate were maintained at 1.0 sccm and 0.9 sccm, respectively. The substrate temperature was kept at 650°C and the growth time was 3 h.

The crystalline properties of the diamond and ZnO nanowires were evaluated by a Bruker-D8 Discover x-ray diffractometer with the CuKα line ($\lambda = 1.54$ Å) as the radiation source. The morphology of the ZnO nanowires was characterized using a Hitachi S-4800 field-emission scanning electron microscope (SEM). The electrical properties of the diamond were measured by a Hall system (LakeShore 7707) under van der Pauw configuration. The photoluminescence (PL) spectra of the ZnO nanowires were recorded under excitation by the 325 nm line of a He–Cd laser. The optically pumped random lasing spectra of the ZnO nanowires were collected by angle-resolved PL spectroscopy under excitation by a 355 nm pulse laser. Electroluminescence (EL) measurements were carried out in a Hitachi F4500 spectrometer using a CW current power source.

3. RESULTS AND DISCUSSION

Figure 1(a) shows the x-ray diffraction (XRD) pattern of the diamond that was employed as a hole source for the random laser. Only one peak can be observed in the pattern and the peak can be indexed to the diffraction from the (111) facet of the diamond. Note that the doublet peaks are the diffractions irradiated by the CuKα1 and Kα2 lines. The strong (111) diffraction peak indicates that the boron-doped diamond is well crystallized. The Raman spectrum of the diamond is shown in Fig. 1(b). Only one sharp peak at around 1331 cm^{-1} with a full width at half-maximum (FWHM) of about 3.4 cm^{-1} can be observed from the spectrum. Generally, the Raman spectrum of undoped diamond is located at 1332 cm^{-1}. The slight shift to the small-wavenumber side of the Raman peak usually results from the incorporation of boron into the lattice of diamond. The microscope image of the

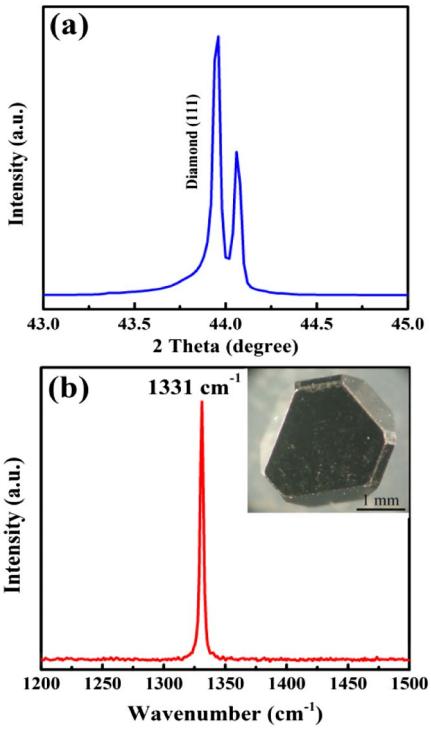

Fig. 1. (a) XRD pattern of the diamond. (b) Raman spectrum of the diamond; the inset is a typical microscope image of the diamond.

diamond is shown in the inset of Fig. 1(b); the (111) face can be observed clearly, which is consistent with the XRD results. The hole concentration and Hall mobility of the diamond as determined by Hall measurement are about 3.6×10^{18} cm^{-3} and 1.5 cm^2/Vs, respectively; the relatively high hole concentration provides a solid ground for the diamond acting as a hole source for electrically pumped random lasers.

To test whether the holes in the diamond can be injected into ZnO-based materials, the boron-doped *p*-type diamond was fastened with *n*-type ZnO films via a direct contact method by a clip. The electron concentration and Hall mobility of the ZnO films are 3.1×10^{19} cm^{-3} and 30 cm^2/Vs, respectively. When a forward bias is applied onto the structure, dominant emission bands at around 397 nm can be observed from the device, as shown in Fig. 2. This emission can be attributed to the near-band-edge (NBE) emission of ZnO. With increase of the injection

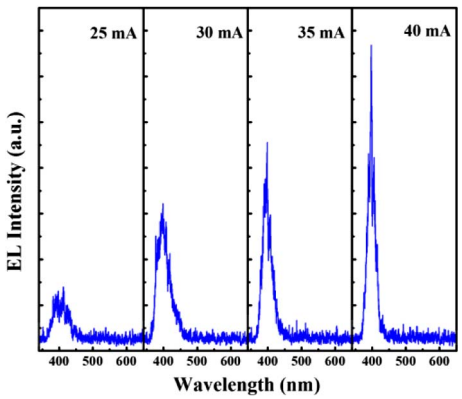

Fig. 2. Room temperature EL spectra of the *n*-type ZnO films fastened onto the *p*-type diamond under different injection currents.

current from 25 to 40 mA, the intensity of the emission increases obviously, which reveals that holes have been injected from the diamond into the ZnO films, and at a larger injection current, more holes are injected; this confirms that the *p*-type diamond can be employed as a hole source for ZnO-based materials.

The structural and optical properties of the ZnO nanowires employed as the active layer for the random lasers are shown in Fig. 3. Besides the diffraction from the *a*-plane sapphire substrate (37.8°), there is only one peak at 34.4° in the XRD pattern of the ZnO nanowires, as shown in Fig. 3(a), which can be indexed to the diffraction from the (0002) facet of wurtzite ZnO. The inset of Fig. 3(a) illustrates the x-ray rocking curve of the nanowires, from which a symmetric Gaussian peak with a FWHM of around 0.49° can be observed. These results indicate that the ZnO nanowires are crystallized in a wurtzite structure with a *c*-axis preferred orientation. A side-view image of the ZnO nanowires is shown in the inset of Fig. 3(b). Well-aligned nanowires grown vertically on the sapphire substrate are visible from the image and the length of the nanowires is about 3.6 μm. The nanowires show a smooth surface, revealing that they are well crystallized. The PL spectrum of the ZnO nanowires is shown in Fig. 3(b). The spectrum shows a sharp peak at around 378 nm, which is the NBE emission of ZnO. The deep-level related emission at around 500 nm is almost undetectable in the spectrum, indicating the relatively high optical quality of the ZnO nanowires.

To test the applicability of the ZnO nanowires as the active layer for random lasing, the optically pumped lasing of the nanowires has been investigated, as shown in Fig. 4(a). Sharp peaks at around 383.7 and 387.2 nm are observed, and the intensities of the peaks increase greatly with the excitation density. Figure 4(b) illustrates the angle-resolved PL spectra of the nanowires, and one can see that the emission intensity of the lasing is distributed over a large angle region (from −30° to 30°), which is a typical characteristic of random lasers, indicating that random lasing has been obtained from the nanowires. The occurrence of optically

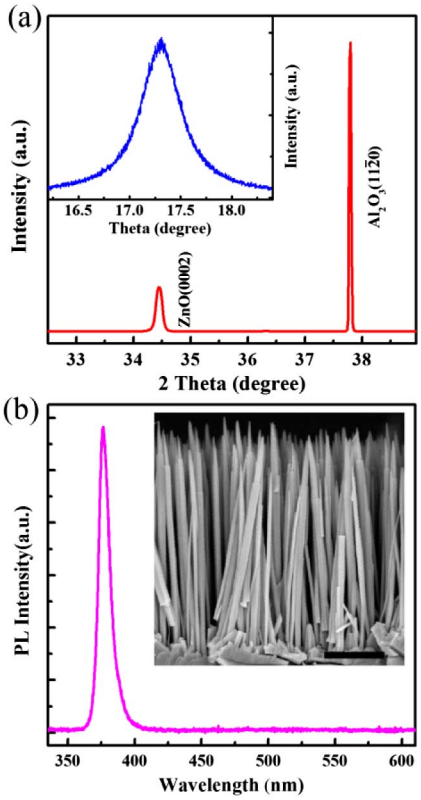

Fig. 3. (a) $\theta - 2\theta$ XRD pattern of the ZnO nanowires; the inset shows the rocking curve of the nanowires. (b) Room temperature PL spectrum of the ZnO nanowires; the inset is a side-view SEM image of the ZnO nanowires and the scale bar is 1 μm.

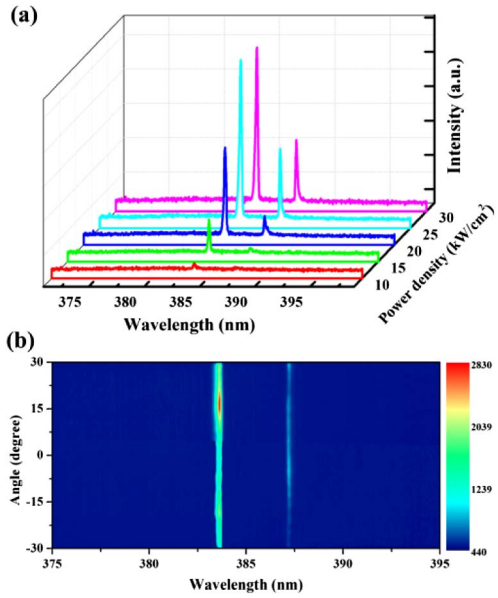

Fig. 4. (a) Optically pumped lasing spectra of the nanowires under different excitation intensities. (b) The angular resolved lasing spectra of the nanowires.

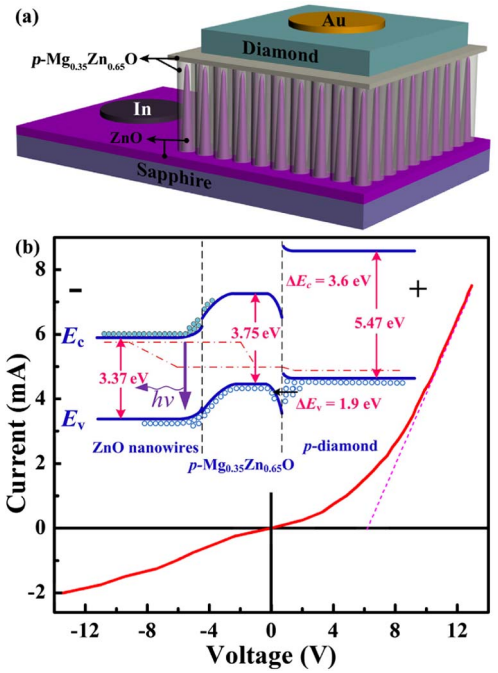

Fig. 5. (a) Schematic illustration of the p-$Mg_{0.35}Zn_{0.65}O$/n-ZnO core–shell nanowire heterostructures with *p*-type diamond as the hole source layer. (b) $I - V$ curve of the device; the inset shows the bandgap diagram of the device under forward bias.

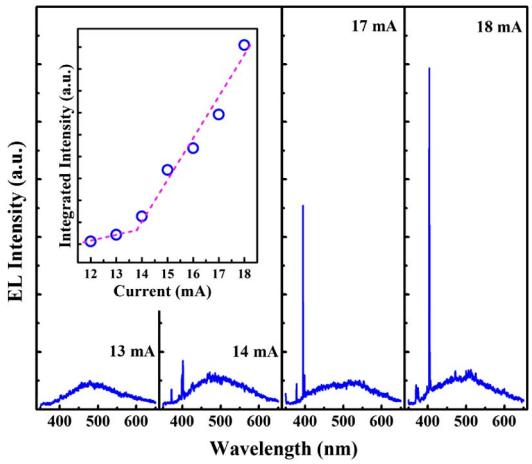

Fig. 6. Room temperature EL spectra of the p-$Mg_{0.35}Zn_{0.65}O$/n-ZnO core–shell nanowire heterostructures with p-type diamond as the hole source layer under different injection currents. The inset shows the dependence of the integrated emission intensity of the device on the injection current.

pumped lasing from the ZnO nanowires reveals that the nanowires can act as the active layer for random lasers.

To achieve electrically pumped random lasers, p-$Mg_{0.35}Zn_{0.65}O$/n-ZnO core–shell nanowire heterostructures have been fabricated by depositing p-type $Mg_{0.35}Zn_{0.65}O$ films onto the nanowires [30], and the core–shell nanowire heterostructures have been bonded together with the p-type diamond via a direct contact method by a clip. A schematic illustration of the structure is shown in Fig. 5(a). The current–voltage (I – V) characteristic of the device shows rectification behavior with a turn-on voltage of around 6.2 V, as shown in Fig. 5(b). The bandgap diagram of the device is shown in the inset of Fig. 5(b). Considering that the electron affinities of $Mg_{0.35}Zn_{0.65}O$ and diamond are 4.0 and 0.38 eV, respectively, and the bandgaps of $Mg_{0.35}Zn_{0.65}O$ and diamond are 3.75 and 5.47 eV, respectively, the conduction band and valence band offsets at the MgZnO–diamond interface can be deduced to be 3.6 and 1.9 eV, respectively. Under forward bias, the conduction and valence bands of the $Mg_{0.35}Zn_{0.65}O$ layer will be bent drastically because of its much larger resistance than diamond and the ZnO nanowires. Thus, a triangle-shaped barrier will be formed at the MgZnO–diamond interface. When the bias is increased, the effective thickness of the triangle barrier will decrease greatly and some holes in the diamond may tunnel through the barrier and enter the $Mg_{0.35}Zn_{0.65}O$ layer. Then the hole concentration in the $Mg_{0.35}Zn_{0.65}O$ layer will be enhanced and the holes in the $Mg_{0.35}Zn_{0.65}O$ layer will be injected into the ZnO nanowires under forward bias. Considering that the ZnO nanowires show n-type conduction, and there are many electrons in this layer, the electrons in the ZnO nanowires will recombine with the holes injected from the diamond and an emission will be produced.

The emission spectra of the p-$Mg_{0.35}Zn_{0.65}O$/n-ZnO core–shell nanowire heterostructure with p-type diamond as a hole source are shown in Fig. 6. One can see that when the injection current is 13 mA, a broad emission with a FWHM of around 138 nm is visible from the spectrum, which is usually attributed to the deep-level related emission of ZnO. When the injection current is increased to 14 mA, two sharp peaks at around 400 nm appear superposed on the broad emission and the FWHMs of the sharp peaks is around 0.9 nm. As the injection current is increased further, the sharp peaks become more predominant. The above phenomenon has been frequently observed in ZnO films and nanostructures and has usually been attributed to the occurrence of lasing [15–17,31,32]. The dependence of the integrated emission intensity on the injection current is shown in the inset of Fig. 6, from which a threshold of about 13.8 mA has been acquired for the lasing. Compared with the PL spectra, the wavelength of the electronically pumped lasing is obviously redshifted, which may be attributed to the heating effect of the device caused by the injection of current. The mechanism of the lasing can be understood as follows: when the emission resulting from the recombination of the electrons in the ZnO nanowires with the holes injected from the diamond is emitted, the photons will encounter strong scattering as they come out of the nanowires. Here the large surface of the nanowires provides an arena for scattering. In some cases, some photons may return to the location from where they are emitted. Under such a circumstance, close loops are formed. At a large injection current, the gain in the close loop may exceed the loss, and thus, lasing will occur. Since the close loops are formed randomly among the nanowires, the emission obtained is random lasing.

4. CONCLUSION

In conclusion, boron-doped p-type diamond has been employed as a hole source for p-$Mg_{0.35}Zn_{0.65}O$/n-ZnO core–shell nanowire heterostructures via a direct contact method and random lasing has been observed from this structure. The lasing results from the recombination of the electrons in the ZnO nanowires and the holes injected from the p-type diamond. The results reported in this article reveal that p-type diamond can be used as a hole source for ZnO, which may provide a promising route to electrically pumped random lasers.

National Natural Science Foundation of China (NSFC) (11134009, 11374296, 11404328, 11464035, 61177040); The National Basic Research Program of China (2011CB302005); The National Science Foundation for Distinguished Young Scholars of China (61425021); The Science and Technology Developing Project of Jilin Province (20111801, 20140101052JC).

REFERENCES

1. S. Gottardo, S. Cavalieri, O. Yaroshchuk, and D. Wiersma, "Quasi-two-dimensional diffusive random laser action," Phys. Rev. Lett. **93**, 263901 (2004).
2. Q. Song, Z. Xu, S. H. Choi, X. Sun, S. Xiao, O. Akkus, and Y. L. Kim, "Detection of nanoscale structural changes in bone using random lasers," Biomed. Opt. Express **1**, 1401–1407 (2010).
3. Q. Song, S. Xiao, Z. Xu, V. M. Shalaev, and Y. L. Kim, "Random laser spectroscopy for nanoscale perturbation sensing," Opt. Lett. **35**, 2624–2626 (2010).
4. D. S. Wiersma and S. Cavalieri, "Light emission: A temperature-tunable random laser," Nature **414**, 708–709 (2001).
5. B. Redding, G. Allen, E. R. Dufresne, and H. Cao, "Low-loss high-speed speckle reduction using a colloidal dispersion," Appl. Opt. **52**, 1168–1172 (2013).
6. D. S. Wiersma, "The physics and applications of random lasers," Nat. Phys. **4**, 359–367 (2008).
7. H. Cao, Y. G. Zhao, H. C. Ong, S. T. Ho, J. Y. Dai, J. Y. Wu, and R. P. H. Chang, "Ultraviolet lasing in resonators formed by scattering in semiconductor polycrystalline films," Appl. Phys. Lett. **73**, 3656–3658 (1998).
8. J. Fallert, R. J. B. Dietz, M. Hauser, F. Stelzl, C. Klingshirn, and H. Kalt, "Random lasing in ZnO nanocrystals," J. Lumin. **129**, 1685–1688 (2009).

9. M. H. Huang, S. Mao, H. Feick, H. Q. Yan, Y. Y. Wu, H. Kind, E. Weber, R. Russo, and P. D. Yang, "Room-temperature ultraviolet nanowire nanolasers," Science **292**, 1897–1899 (2001).
10. R. Chen, Q. L. Ye, T. He, V. D. Ta, Y. Ying, Y. Y. Tay, T. Wu, and H. Sun, "Exciton localization and optical properties improvement in nanocrystal-embedded ZnO core-shell nanowires," Nano Lett. **13**, 734–739 (2013).
11. J. Fallert, R. J. B. Dietz, J. Sartor, D. Schneider, C. Klingshirn, and H. Kalt, "Co-existence of strongly and weakly localized random laser modes," Nat. Photonics **3**, 279–282 (2009).
12. C. H. Liu, J. A. Zapien, Y. Yao, X. M. Meng, C. S. Lee, S. S. Fan, Y. Lifshitz, and S. T. Lee, "High-density, ordered ultraviolet light-emitting ZnO nanowire arrays," Adv. Mater. **15**, 838–841 (2003).
13. S. P. Lau, H. Yang, S. F. Yu, C. Yuen, E. S. P. Leong, H. Li, and H. H. Hng, "Flexible ultraviolet random lasers based on nanoparticles," Small **1**, 956–959 (2005).
14. A. B. Djurišić and Y. H. Leung, "Optical properties of ZnO nanostructures," Small **2**, 944–961 (2006).
15. H. Zhu, C. X. Shan, B. Yao, B. H. Li, J. Y. Zhang, Z. Z. Zhang, D. X. Zhao, D. Z. Shen, X. W. Fan, Y. M. Lu, and Z. K. Tang, "Ultralow-threshold laser realized in zinc oxide," Adv. Mater. **21**, 1613–1617 (2009).
16. H. Zhu, C. X. Shan, J. Y. Zhang, Z. Z. Zhang, B. H. Li, D. X. Zhao, B. Yao, D. Z. Shen, X. W. Fan, Z. K. Tang, X. Hou, and K. L. Choy, "Low-threshold electrically pumped random lasers," Adv. Mater. **22**, 1877–1881 (2010).
17. J. Huang, S. Chu, J. Y. Kong, L. Zhang, C. M. Schwarz, G. P. Wang, L. Chernyak, Z. H. Chen, and J. L. Liu, "ZnO p-n homojunction random laser diode based on nitrogen-doped p-type nanowires," Adv. Opt. Mater. **1**, 179–185 (2013).
18. J. C. Fan, K. M. Sreekanth, Z. Xie, S. L. Chang, and K. V. Rao, "p-Type ZnO materials: theory, growth, properties and devices," Prog. Mater. Sci. **58**, 874–985 (2013).
19. A. Tsukazaki, A. Ohtomo, T. Onuma, M. Ohtani, T. Makino, M. Sumiya, K. Ohtani, S. F. Chichibu, S. Fuke, Y. Segawa, H. Ohno, H. Koinuma, and M. Kawasaki, "Repeated temperature modulation epitaxy for p-type doping and light-emitting diode based on ZnO," Nat. Mater. **4**, 42–46 (2004).
20. D. C. Look, D. C. Reynolds, C. W. Litton, R. L. Jones, D. B. Eason, and G. Cantwell, "Characterization of homoepitaxial p-type ZnO grown by molecular beam epitaxy," Appl. Phys. Lett. **81**, 1830 (2002).
21. J. Isberg, J. Hammersberg, E. Johansson, T. Wikstrom, D. J. Twitchen, A. J. Whitehead, S. E. Coe, and G. A. Scarsbrook, "High carrier mobility in single-crystal plasma-deposited diamond," Science **297**, 1670–1672 (2002).
22. C. J. H. Wort and R. S. Balmer, "Diamond as an electronic material," Mater. Today **11**(1–2), 22–28 (2008).
23. R. S. Balmer, J. R. Brandon, S. L. Clewes, H. K. Dhillon, J. M. Dodson, I. Friel, P. N. Inglis, T. D. Madgwick, M. L. Markham, T. P. Mollart, N. Perkins, G. A. Scarsbrook, D. J. Twitchen, A. J. Whitehead, J. J. Wilman, and S. M. Woollard, "Chemical vapour deposition synthetic diamond: materials, technology and applications," J. Phys. Condens. Matter **21**, 364221 (2009).
24. I. Aharonovich, A. D. Greentree, and S. Prawer, "Diamond photonics," Nat. Photonics **5**, 397–405 (2011).
25. V. S. Bormashov, S. A. Tarelkin, S. G. Buga, M. S. Kuznetsov, S. A. Terentiev, A. N. Semenov, and V. D. Blank, "Electrical properties of the high quality boron-doped synthetic single-crystal diamonds grown by the temperature gradient method," Diam. Relat. Mater. **35**, 19–23 (2013).
26. Y. Li, X. Jia, H. A. Ma, J. Zhang, F. Wang, N. Chen, and Y. Feng, "Electrical properties of diamond single crystals co-doped with hydrogen and boron," CrystEngComm **16**, 7547–7551 (2014).
27. J. S. Liu, C. X. Shan, B. H. Li, Z. Z. Zhang, K. W. Liu, and D. Z. Shen, "MgZnO p-n heterostructure light-emitting devices," Opt. Lett. **38**, 2113–2115 (2013).
28. J. S. Liu, C. X. Shan, H. Shen, B. H. Li, Z. Z. Zhang, L. Liu, L. G. Zhang, and D. Z. Shen, "ZnO light-emitting devices with a lifetime of 6.8 hours," Appl. Phys. Lett. **101**, 011106 (2012).
29. X. Y. Liu, C. X. Shan, C. Jiao, S. P. Wang, H. F. Zhao, and D. Z. Shen, "Pure ultraviolet emission from ZnO nanowire-based p-n heterostructures," Opt. Lett. **39**, 422–425 (2014).
30. Y. J. Lu, C. X. Shan, M. M. Jiang, G. C. Hu, N. Zhang, S. P. Wang, B. H. Li, and D. Z. Shen, "Random lasing realized in n-ZnO/p-MgZnO core-shell nanowire heterostructures," CrystEngComm **17**, 3917–3922 (2015).
31. X. Y. Ma, P. L. Chen, D. S. Li, Y. Y. Zhang, and D. R. Yang, "Electrically pumped ZnO film ultraviolet random lasers on silicon substrate," Appl. Phys. Lett. **91**, 251109 (2007).
32. X. Y. Ma, J. W. Pan, P. L. Chen, D. S. Li, H. Zhang, Y. Yang, and D. R. Yang, "Room temperature electrically pumped ultraviolet random lasing from ZnO nanorod arrays on Si," Opt. Express **17**, 14426–14433 (2009).